

# Reinforcement Graph Clustering with Unknown Cluster Number

Yue Liu

Email:yueliu19990731@163.com

NUDT

Changsha, Hunan, China

Ke Liang

NUDT

Changsha, Hunan, China

Jun Xia

Westlake University

Hangzhou, Zhejiang, China

Xihong Yang

NUDT

Changsha, Hunan, China

Sihang Zhou

NUDT

Changsha, Hunan, China

Meng Liu

NUDT

Changsha, Hunan, China

Xinwang Liu\*

NUDT

Changsha, Hunan, China

Stan Z. Li

Westlake University

Hangzhou, Zhejiang, China

## ABSTRACT

Deep graph clustering, which aims to group nodes into disjoint clusters by neural networks in an unsupervised manner, has attracted great attention in recent years. Although the performance has been largely improved, the excellent performance of the existing methods heavily relies on an accurately predefined cluster number, which is not always available in the real-world scenario. To enable the deep graph clustering algorithms to work without the guidance of the predefined cluster number, we propose a new deep graph clustering method termed Reinforcement Graph Clustering (RGC). In our proposed method, cluster number determination and unsupervised representation learning are unified into a uniform framework by the reinforcement learning mechanism. Concretely, the discriminative node representations are first learned with the contrastive pretext task. Then, to capture the clustering state accurately with both local and global information in the graph, both node and cluster states are considered. Subsequently, at each state, the qualities of different cluster numbers are evaluated by the quality network, and the greedy action is executed to determine the cluster number. In order to conduct feedback actions, the clustering-oriented reward function is proposed to enhance the cohesion of the same clusters and separate the different clusters. Extensive experiments demonstrate the effectiveness and efficiency of our proposed method. The source code of RGC is shared at <https://github.com/yueliu1999/RGC> and a collection (papers, codes and, datasets) of deep graph clustering is shared at <https://github.com/yueliu1999/Awesome-Deep-Graph-Clustering> on Github.

\*Corresponding author

Permission to make digital or hard copies of all or part of this work for personal or classroom use is granted without fee provided that copies are not made or distributed for profit or commercial advantage and that copies bear this notice and the full citation on the first page. Copyrights for components of this work owned by others than the author(s) must be honored. Abstracting with credit is permitted. To copy otherwise, or republish, to post on servers or to redistribute to lists, requires prior specific permission and/or a fee. Request permissions from [permissions@acm.org](mailto:permissions@acm.org).

MM '23, October 29–November 3, 2023, Ottawa, ON, Canada

© 2023 Copyright held by the owner/author(s). Publication rights licensed to ACM.

ACM ISBN 979-8-4007-0108-5/23/10...\$15.00

<https://doi.org/10.1145/3581783.3612155>

## KEYWORDS

Attribute Graph Clustering, Unknown Cluster Number, Reinforcement Learning, Graph Neural Network

## ACM Reference Format:

Yue Liu, Ke Liang, Jun Xia, Xihong Yang, Sihang Zhou, Meng Liu, Xinwang Liu, and Stan Z. Li. 2023. Reinforcement Graph Clustering with Unknown Cluster Number. In *Proceedings of the 31st ACM International Conference on Multimedia (MM '23)*, October 29–November 3, 2023, Ottawa, ON, Canada. ACM, New York, NY, USA, 10 pages. <https://doi.org/10.1145/3581783.3612155>

## 1 INTRODUCTION

In recent years, multimedia techniques have witnessed great success in many domains, like vision [14, 68], language, and graphs. Among various research directions, deep graph clustering is an important unsupervised-learning task to encode nodes in the graph with deep neural networks and separates them into different groups. Motivated by the great success of the graph neural networks [19, 20, 57] in different areas, such as recommendation [63], knowledge graph [28–30], and drug prediction [62], anomaly detection [7, 8], and code search [41], deep graph clustering methods have been increasingly proposed in recent years. Although achieving promising performance, the recent deep graph clustering algorithms [31, 33, 37, 38, 58, 70] are parametric, i.e., requiring the input of predefined cluster number, which is not always available in the real scenario.

In the field of traditional clustering [23, 24, 60, 71], several cluster number estimation methods [21] like ELBOW [44] can be optional to determine the cluster number based on the unsupervised criterion. However, they bring heavy computational costs to deep graph clustering methods since the neural network needs to be repeatedly trained with different cluster numbers and search for the best choice. Experimental evidence can be found in Section 4.4.

To solve this open problem, a novel deep graph clustering method termed Reinforcement Graph Clustering (RGC) is proposed by learning the cluster number with the reinforcement learning mechanism. Our proposed RGC unifies cluster number determination and unsupervised representation learning into the reinforcement learning framework. Concretely, the nodes are first embedded with the self-supervised encoder, thus improving the discriminative capability of

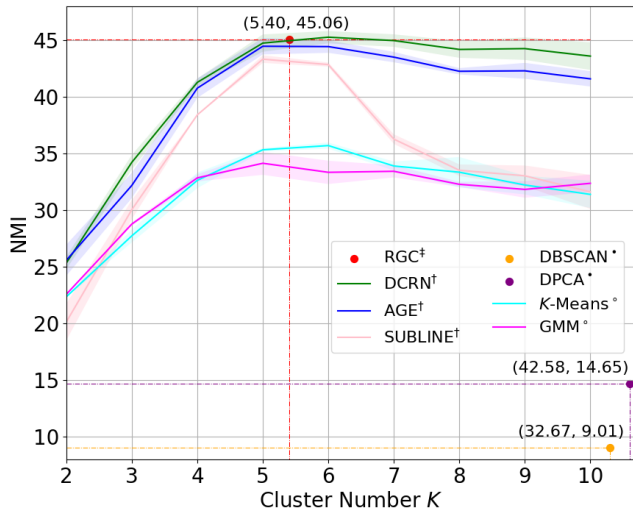


**Figure 1: Clustering performance comparison on CITE-SEER dataset. Four categories of the competitors include traditional parametric methods<sup>°</sup> [12, 51], traditional non-parametric methods<sup>\*</sup> [9, 52], deep parametric methods<sup>†</sup> [6, 35, 39], and deep non-parametric method<sup>‡</sup> (our proposed RGC). For the parametric methods, the results are obtained with the different cluster numbers  $K \in [2, 10]$ .**

samples. Then, we model the process of determining cluster number as a Markov decision process. To capture the states accurately with both the local and global information in the graph, both node and cluster states are considered. Then, at each state, the designed quality network learns the quality of different cluster numbers, and the greedy action is executed to determine the cluster number. For feedback actions, a clustering-oriented reward function is proposed to enhance the cohesion of the same clusters while separating the different clusters. With the experience replay strategy, the quality network is trained by minimizing the reinforcement learning loss. With these settings, our proposed RGC can automatically determine the cluster number and achieve comparable performance. To demonstrate the effectiveness of our proposed RGC, we conduct experiments as shown in Figure 1 and conclude as follows. Firstly, benefiting from the strong unsupervised representation capability of RGC, it significantly outperforms the non-deep parametric/non-parametric methods [9, 12, 51, 52]. Besides, in the reinforcement learning framework, our non-parametric deep method RGC is endowed with the cluster number determination capability, thus achieving comparable performance to the deep parametric methods [6, 35, 39]. The main contributions of this work are summarized as follows.

- We find the promising performance of recent deep graph clustering methods relies on the predefined cluster number and a new non-parametric deep graph clustering method is proposed.
- We unify the cluster number determination and the unsupervised learning into a uniform framework by the reinforcement learning mechanism.

- A clustering-orient reward function is proposed to guide the network to enhance the cohesion of the same clusters and separate the different clusters.
- Extensive experimental results on five benchmark datasets demonstrate the effectiveness and efficiency of our proposed RGC.

## 2 RELATED WORK

### 2.1 Deep Graph Clustering

Attribute graph clustering, which aims to group the nodes in the graph into disjoint clusters, is a fundamental and challenging task. In recent years, benefiting from the strong structural representation capability of graph neural networks [19, 20, 42, 57, 69], deep graph clustering methods [1, 35, 37, 40, 55] achieve promising performance. According to the learning mechanism, the mainstream methods can be roughly categorized into three classes, i.e., generative methods [1, 5, 25, 26, 32, 43, 48, 50, 58, 59, 65, 72], adversarial methods [10, 46, 47, 54], and contrastive methods [6, 13, 34, 35, 37, 40, 49, 64, 73]. Refer to the survey of deep graph clustering [36]. However, these methods are parametric, i.e., requiring the predefined cluster number  $K$ . Besides, as shown in Figure 1 and Figure 5, we observe that the wrong cluster number  $K$  will lead to unpromising performance. Although in the field of traditional clustering, several  $K$  estimation methods [21] like ELBOW [44] can help researchers to choose the cluster number, they will bring expensive computational costs since the deep neural networks need to be trained for repeated times. The experimental evidence can be found in Figure 4. To solve the problem, we propose a novel deep graph clustering method termed Reinforcement Graph Clustering (RGC) to automatically determine the cluster number  $K$  by reinforcement learning. RGC is the first non-parametric deep graph clustering method. Through extensive experiments, we demonstrate that RGC can save training time compared with the  $K$  estimation methods and achieves comparable performance to the state-of-the-art parametric deep graph clustering methods.

### 2.2 Non-parametric Clustering and Cluster Number Estimation

In the clustering task, the correct number of clusters is not always known in practice. Thus, there are two alternative options, i.e., cluster number estimation methods or non-parametric clustering methods. The cluster number estimation methods can help to determine the cluster number by performing multiple clustering runs and selecting the best cluster number based on the unsupervised criterion. The mainstream cluster number estimation methods [21] include thumb rule, ELBOW [44],  $t$ -SNE [56], etc. The thumb rule simply assigns the cluster number  $K$  with  $\sqrt{N/2}$ , where  $N$  is the number of samples. This manual setting is empirical and can not be applicable to all datasets. Besides, the ELBOW is a visual method. Concretely, they start the cluster number  $K = 2$  and keep increasing  $K$  in each step by 1, calculating the WSS (within-cluster sum of squares) during training. They choose the value of  $K$  when the WSS drops dramatically and after that, it reaches a plateau. However, it will bring large computational costs since the deep neural network needs to be trained with repeated times. Another visual method termed  $t$ -SNE visualizes the high-dimension data into 2D

sample points and helps researchers to determine the cluster number. The effectiveness of  $t$ -SNE heavily relies on the experience of researchers. Differently, several non-parametric clustering methods, which are free from inputting the cluster number  $K$ , have been proposed in the field of the traditional clustering [9, 52] and deep clustering [53]. However, they are not suitable for the graphs since they neglect structural information. Besides, there are few deep non-parametric graph clustering methods. From this motivation, we focus on making deep graph clustering methods work without the guidance of the predefined cluster number.

### 3 REINFORCEMENT GRAPH CLUSTERING

In this section, we propose a novel deep graph clustering method termed Reinforcement Graph Clustering (RGC) to enable the deep graph clustering algorithm to work without the guidance of the predefined cluster number. In RGC, a cluster number learning module is designed based on reinforcement learning to automatically determine the cluster number. Besides, the discriminative node representations are learned in a self-supervised manner. By these settings, RGC can intelligently determine the cluster number and achieve promising clustering performance. The overall framework is demonstrated in Figure 2. In the following sections, we will introduce the notations, define the problem, and detail the proposed RGC.

#### 3.1 Notation and Problem

In this paper,  $\mathcal{V} = \{v_1, v_2, \dots, v_N\}$  denotes as the node set of  $N$  nodes with  $K$  classes. Besides,  $\mathcal{E}$  denotes a set of edges in the graph  $\mathcal{G} = \{\mathcal{V}, \mathcal{E}\}$ . In the matrix form,  $\mathbf{X} \in \mathbb{R}^{N \times D}$  and  $\mathbf{A} \in \mathbb{R}^{N \times N}$  denotes the attribute matrix and the original adjacency matrix, respectively. The notations are summarized in Table 1. The target of deep graph clustering is to encode nodes with neural networks  $\mathcal{F}$  in an unsupervised manner and then divide them into several disjoint clusters. In the existing deep graph clustering methods, the promising performance heavily relies on the precisely predefined cluster number  $K$ , which is not always known in the real scenario. Thus, this work focuses on making the deep graph clustering method work without the guidance of the predefined cluster number  $K$ .

#### 3.2 Encoding

Firstly, we encode the nodes to the embeddings  $\mathbf{Z} \in \mathbb{R}^{N \times d}$  with the encoder  $\mathcal{F}$  as follow:

$$\mathbf{Z} = \mathcal{F}(\mathbf{X}, \mathbf{A}), \quad (1)$$

where  $\mathbf{X}$  and  $\mathbf{A}$  denote the attribute matrix and adjacency matrix, respectively. The detailed designation of  $\mathcal{F}$  is described in Appendix A.1. The encoder is trained self-supervised. Concretely, the encoder loss  $\mathcal{L}_{\mathcal{F}}$  contains the contrastive loss and the clustering loss described in Section 3.4. After encoding, the clustering algorithm  $\mathcal{P}$  will be performed on  $\mathbf{Z}$  and obtain the clustering results as follow:

$$\mathbf{C}, \mathbf{P} = \mathcal{P}(\mathbf{Z}, \hat{K}), \quad (2)$$

Notation	Meaning
$\mathbf{X} \in \mathbb{R}^{N \times D}$	Attribute matrix
$\mathbf{A} \in \mathbb{R}^{N \times N}$	Original adjacency matrix
$\mathbf{L} \in \mathbb{R}^{N \times N}$	Graph Laplacian matrix
$\mathbf{Z} \in \mathbb{R}^{N \times d}$	Node embeddings
$\mathbf{C} \in \mathbb{R}^{\hat{K} \times d}$	Cluster embeddings
$\mathbf{Z}_t \in \mathbb{R}^{N \times d}$	Node state at epoch $t$
$\mathbf{C}_t \in \mathbb{R}^{\hat{K} \times d}$	Cluster state at epoch $t$
$\hat{K}_t \in \mathbb{R}$	Learned cluster number at epoch $t$
$\mathbf{S}_t = \{\mathbf{Z}_t, \mathbf{C}_t\}$	State at epoch $t$
$\mathbf{q}_t \in \mathbb{R}^{N^K}$	Quality score at epoch $t$
$R_t \in \mathbb{R}$	Reward at epoch $t$
$\mathcal{F}$	Sample Encoder Network
$\mathcal{Q}$	Quality Network
$\pi$	Policy with $\epsilon$ -greedy

Table 1: Basic notation summary.

where  $\hat{K}$  denotes the learned cluster number and  $\mathbf{P} \in \mathbb{R}^{N \times \hat{K}}$  denotes the cluster assignment matrix. Besides, the cluster embeddings  $\mathbf{C} \in \mathbb{R}^{\hat{K} \times d}$  are calculated by averaging the node embeddings within each cluster. In the next section, we detail the process of learning cluster number  $\hat{K}$ .

#### 3.3 Cluster Number Learning Module

In this section, the cluster number learning module is proposed based on reinforcement learning. Firstly, the cluster number determination is modelled as the Markov decision process during training. Four important elements in the Markov decision process, including state, action, transition, and reward, are defined as follows.

- **State.** In order to capture the local and global information in the graph, the state  $\mathbf{S}_t$  at  $t$  epoch are built with both the node representations and the cluster representations. Formally, the states are formulated as follows:

$$\mathbf{S}_t = \{\mathbf{Z}_t, \mathbf{C}_t\}, \quad (3)$$

where  $\mathbf{C}_t \in \mathbb{R}^{\hat{K} \times d}$  is calculated by averaging the node embeddings within each cluster. In this manner, the states will contain both the node and cluster information, better revealing the potential semantics in the graph.

- **Transition.** The state  $\mathbf{S}_t = \{\mathbf{Z}_t, \mathbf{C}_t\}$  will be transitioned to  $\mathbf{S}_{t+1} = \{\mathbf{Z}_{t+1}, \mathbf{C}_{t+1}\}$  in the process of training. Concretely, when the training epoch number increases, the encoder  $\mathcal{F}$  will be optimized by minimizing encoder loss  $\mathcal{L}_{\mathcal{F}}$ , leading to a state transition.
- **Action.** To evaluate the quality of different cluster numbers, the quality network is carefully designed as follows:

$$\mathbf{q}_t = \mathcal{Q}(\mathbf{S}_t) = \mathcal{Q}(\{\mathbf{Z}_t, \mathbf{C}_t\}), \quad (4)$$

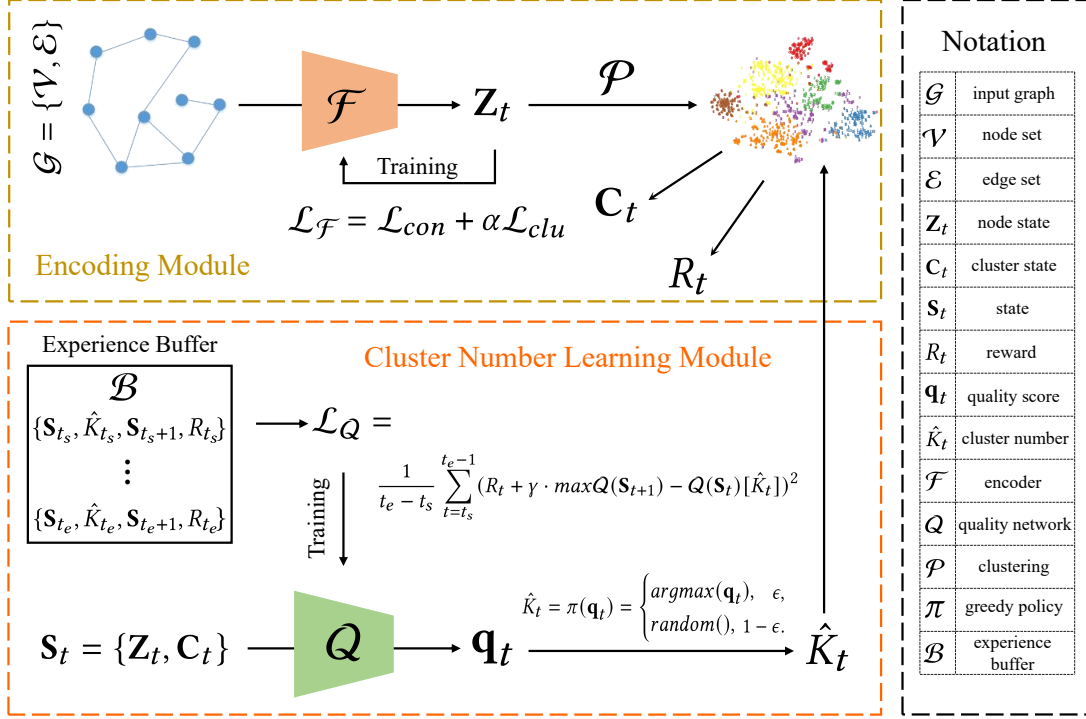


**Figure 2: Reinforcement Graph Clustering (RGC).** In a graph  $\mathcal{G}$ , the nodes are encoded with  $\mathcal{F}$ , which is trained in a self-supervised manner, thus improving the discriminative capability of samples. Then, to capture local and global information, state  $\mathbf{S}_t$  is built with both node and cluster states. In addition, the quality network  $Q$  is designed to evaluate cluster numbers (actions) at  $\mathbf{S}_t$  and take the greedy action under policy  $\pi$ . Moreover, a clustering-oriented reward  $R_t$  is proposed to improve the cohesion of the same clusters while separating different clusters. With the experience buffer  $\mathcal{B}$ ,  $Q$  is trained by minimizing  $\mathcal{L}_Q$ . By these settings, our RGC can intelligently determine the cluster number and achieve promising clustering performance.

where  $\mathbf{q}_t \in \mathbb{R}^{N_k}$  denotes the quality score vector and  $\mathbf{q}_t[i]$  indicates the quality of cluster number  $i$ . Besides,  $N_k$  is the max cluster number. Based on  $\mathbf{q}_t$ , the cluster number is estimated as follows:

$$\hat{K}_t = \pi(\mathbf{q}_t) = \begin{cases} \operatorname{argmax}(\mathbf{q}_t), & \epsilon, \\ \operatorname{random}(), & 1 - \epsilon. \end{cases} \quad (5)$$

Here, the  $\epsilon$ -greedy strategy is adopted. To be precise, under the policy  $\pi$ ,  $Q$  takes the greedy action with the probability  $\epsilon$  and random decision with the probability  $1 - \epsilon$ . The greedy parameter  $\epsilon$  increases as the training epoch number increases, guiding the policy  $\pi$  to take intelligent decision with higher probability. In this way, our proposed method RGC can evaluate different cluster numbers and takes the intelligent decision during training. The detailed designation of the quality network can be found in Appendix A.3.

- **Reward.** After taking an action at state  $\mathbf{S}_t$ , the reward function will feedback to the network. In our proposed RGC, for the clustering task, a clustering-oriented reward function  $\mathcal{R}$  is proposed as follows.

$$R_t = \mathcal{R}(\mathbf{S}_t, \hat{K}_t) = \mathcal{R}(\{\mathbf{Z}_t, \mathbf{C}_t\}, \hat{K}_t) = -\frac{1}{N} \sum_i \min_j \mathcal{D}(\mathbf{Z}_t[i], \mathbf{C}_t[j]) + \frac{1}{\hat{K}^2} \sum_i \sum_j \mathcal{D}(\mathbf{C}_t[i], \mathbf{C}_t[j]), \quad (6)$$

where  $\mathcal{D}$  denotes the distance metric function like Euclidean distance. During training, our quality network is encouraged to maximize the reward  $R_t \in \mathbb{R}$ . Through  $\max R_t$ , the first term in Eq. (6) minimizes the distance between each node and the corresponding cluster center while the second term in Eq. (6) maximizes the distance between different cluster centers. Guided by the clustering-oriented reward function, the proposed RGC can improve cohesion in the same clusters while separating different clusters.

In these settings, the Markov decision process of determining the cluster number is constructed. Subsequently, the experiences are collected by the experience replay strategy and the quality network is trained by minimizing the reinforcement loss. In the next section, we detail the training of our proposed method.

### 3.4 Training

In this section, we introduce the training technique of the proposed RGC. It mainly contains two parts including encoding network training and quality network training.

To train the encoder  $\mathcal{F}$  in a self-supervised manner, we construct a contrastive pre-text task. Specifically, two-view node embeddings are generated and the network is forced to pull together the same nodes in different views while pushing away the different ones. The

**Table 2: Clustering performance of the state-of-the-art deep parametric methods <sup>†</sup> and our proposed deep non-parametric method RGC<sup>‡</sup>. All results are obtained by ten runs and reported with mean±std (%). The bold and underlined result denotes the champion and runner-up.**

Method	BAT		EAT		AMAP		CITSEER		CORA		
	NMI	ARI	NMI	ARI	NMI	ARI	NMI	ARI	NMI	ARI	
DEC <sup>†</sup>	ICML'16	14.10±1.99	07.99±1.21	04.96±1.74	03.60±1.87	37.35±0.05	18.59±0.04	28.34±0.30	28.12±0.36	23.54±0.34	15.13±0.42
DCN <sup>†</sup>	ICML'17	18.03±7.73	13.75±6.05	06.92±2.80	05.11±2.65	38.76±0.30	20.80±0.47	27.64±0.08	29.31±0.14	25.65±0.65	21.63±0.58
IDEC <sup>†</sup>	IJCAI'17	12.80±1.74	07.85±1.31	04.63±0.97	03.19±0.76	37.83±0.08	19.24±0.07	27.17±2.40	25.70±2.65	26.31±1.22	22.07±1.53
AdaGAE <sup>†</sup>	TPAMI'21	15.84±0.78	07.80±0.41	04.36±1.87	02.47±0.54	55.96±0.87	46.20±0.45	27.79±0.47	24.19±0.85	32.19±1.34	28.25±0.98
MGAE <sup>†</sup>	CIKM'17	30.59±2.06	24.15±1.70	20.69±0.98	18.33±1.79	62.13±2.79	48.82±4.57	34.63±0.65	33.55±1.18	28.78±2.97	16.43±1.65
DAEGC <sup>†</sup>	IJCAI'19	21.43±0.35	18.18±0.29	21.33±0.44	20.50±0.51	65.25±0.45	58.12±0.24	36.41±0.86	37.78±1.24	52.89±0.69	49.63±0.43
ARGA <sup>†</sup>	IJCAI'19	<u>49.09±0.54</u>	<u>42.02±1.21</u>	25.44±0.31	16.57±0.31	58.36±2.76	44.18±4.41	34.40±0.71	34.32±0.70	51.06±0.52	47.71±0.33
SDCN <sup>†</sup>	WWW'20	25.74±5.71	21.04±4.97	21.61±1.26	21.63±1.49	44.85±0.83	31.21±1.23	38.71±0.32	40.17±0.43	14.28±1.91	07.78±3.24
AGE <sup>†</sup>	KDD'20	36.04±1.54	26.59±1.83	23.64±0.66	20.39±0.70	65.38±0.61	55.89±1.34	44.93±0.53	45.31±0.41	<u>57.58±1.42</u>	<u>50.10±2.14</u>
MVGRL <sup>†</sup>	ICML'20	29.33±0.70	13.45±0.03	21.53±0.94	17.12±1.46	30.28±3.94	18.77±2.34	40.69±0.93	34.18±1.24	55.57±1.54	48.70±3.94
DFCN <sup>†</sup>	AAAI'21	48.77±0.51	37.76±0.23	<u>26.49±0.41</u>	11.87±0.23	66.23±1.21	58.28±0.74	43.90±0.20	45.50±0.30	19.36±0.87	04.67±2.10
GDCL <sup>†</sup>	IJCAI'21	31.70±0.42	19.33±0.57	25.10±0.01	<u>21.76±0.01</u>	37.32±0.28	21.57±0.51	39.52±0.38	41.07±0.96	56.60±0.36	48.05±0.72
GCA <sup>†</sup>	WWW'21	38.88±0.23	26.69±2.85	24.05±0.25	14.37±0.19	48.38±2.38	26.85±0.44	36.15±0.78	35.20±0.96	46.87±0.65	30.32±0.98
MGC <sup>†</sup>	NIPS'21	23.11±0.56	8.41±0.32	16.64±0.41	12.21±0.13	OOM		39.11±0.06	37.54±0.12	24.11±1.00	14.33±1.26
AutoSSL <sup>†</sup>	ICLR'22	17.84±0.98	13.11±0.81	17.86±0.22	13.13±0.71	48.56±0.71	26.87±0.34	40.67±0.84	38.73±0.55	47.62±0.45	38.92±0.77
AGC-DRR <sup>†</sup>	IJCAI'22	19.91±0.24	14.59±0.13	11.15±0.24	09.50±0.25	<u>66.54±1.24</u>	<b>60.15±1.56</b>	43.28±1.41	45.34±2.33	18.74±0.73	14.80±1.64
DCRN <sup>†</sup>	AAAI'22	47.23±0.74	39.76±0.87	24.09±0.53	17.17±0.69	OOM		<b>45.86±0.35</b>	<b>47.64±0.30</b>	45.13±1.57	33.15±0.14
AFGRL <sup>†</sup>	AAAI'22	27.55±0.62	21.89±0.74	17.33±0.54	13.62±0.57	64.05±0.15	54.45±0.48	15.17±0.47	14.32±0.78	12.36±1.54	14.32±1.87
ProGCL <sup>†</sup>	ICML'22	28.69±0.92	21.84±1.34	22.04±2.23	14.74±1.99	39.56±0.39	34.18±0.89	39.59±0.39	36.16±1.11	41.02±1.34	30.71±2.70
SUBLIME <sup>†</sup>	WWW'22	22.03±0.48	14.45±0.87	21.85±0.62	19.51±0.45	06.37±1.89	05.36±2.14	43.15±0.14	44.21±0.54	53.88±1.02	<b>50.15±0.14</b>
RGC <sup>‡</sup>	Ours	<b>51.58±0.83</b>	<b>47.16±1.35</b>	<b>37.77±0.13</b>	<b>30.16±0.15</b>	<b>69.61±0.36</b>	<b>59.58±0.39</b>	<u>45.06±0.93</u>	<u>46.17±1.46</u>	<b>57.60±1.36</b>	49.46±2.72

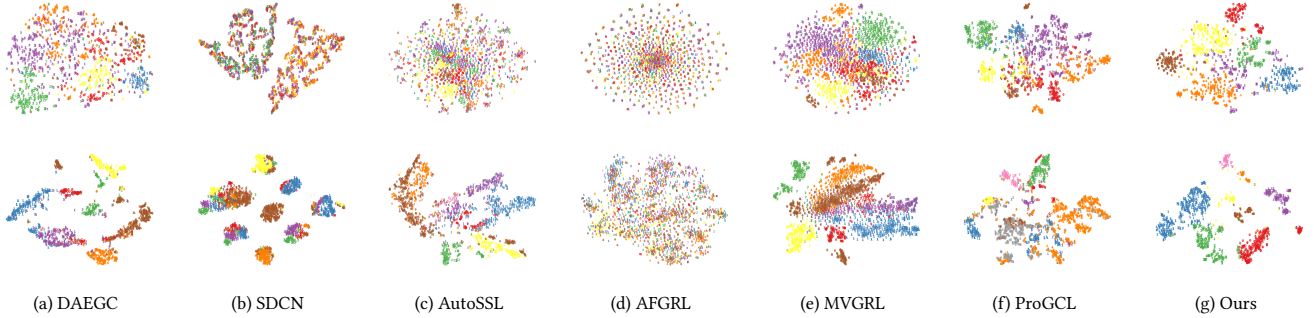


**Figure 3: 2D  $t$ -SNE visualization of seven methods on two benchmark datasets. The first row and second row corresponds to CORA and AMAP dataset, respectively.**

contrastive loss  $\mathcal{L}_{con}$  is formulated as the infoNCE loss. In addition, a clustering guidance loss  $\mathcal{L}_{clu}$  is adapted to align the clustering distribution with the sharpened ones. The detailed formulations of  $\mathcal{L}_{con}$  and  $\mathcal{L}_{clu}$  can be found in Appendix A.2. Thus, the encoder loss is formulated as  $\mathcal{L}_{\mathcal{F}} = \mathcal{L}_{con} + \alpha \mathcal{L}_{clu}$ , where  $\alpha$  is the trade-off hyper-parameter.

For the  $Q$  network training, the experience replay training strategy is adopted. Concretely, during training, we will collect the experience quadruple tuples including states, actions, next states, and rewards into the experience buffer  $\mathcal{B}$  as follow.

$$\mathcal{B} = \{\mathbf{S}_t, \hat{K}_t, \mathbf{S}_{t+1}, R_t | t \in [t_s, t_e]\}, \quad (7)$$

where  $t_s$  and  $t_e$  are the start epoch and the end epoch of the collection. Based on the collected experience buffer  $\mathcal{B}$ , the quality

network  $Q$  will be trained by minimizing the following reinforcement learning loss:

$$\mathcal{L}_Q = \frac{1}{t_e - t_s} \sum_{t=t_s}^{t_e-1} (R_t + \gamma \cdot \max \mathbf{q}_{t+1} - \mathbf{q}_t [\hat{K}_t])^2 = \frac{1}{t_e - t_s} \sum_{t=t_s}^{t_e-1} (R_t + \gamma \cdot \max Q(\mathbf{S}_{t+1}) - Q(\mathbf{S}_t) [\hat{K}_t])^2, \quad (8)$$

where  $\gamma$  is a discount factor for the future step. In Eq. (8), the term  $R_t + \gamma \cdot \max Q(\mathbf{S}_{t+1})$  is the quality estimation of action  $\hat{K}_t$  at state  $\mathbf{S}_t$ . Besides, the term  $Q(\mathbf{S}_t) [\hat{K}_t]$  is the learned quality of action  $\hat{K}_t$  at state  $\mathbf{S}_t$ . By minimizing  $\mathcal{L}_Q$ ,  $Q$  is guided to better learn the quality of actions and take intelligent action.

In summary, the encoder network is trained by minimizing the encoder loss  $\mathcal{L}_{\mathcal{F}}$  and the quality network  $Q$  is optimized by minimizing the reinforcement learning loss  $\mathcal{L}_Q$ . By these settings, our

proposed RGC is endowed with strong representation capability and cluster number recognition capability, thus achieving promising performance.

### 3.5 Complexity Analysis

In this section, we analyze the time and space complexity of calculating the loss functions in our proposed RGC. Assume that the max cluster number, the experience buffer size, and the encoding time for one state is  $N_K$ ,  $N_B$ , and  $T_{\mathcal{F}}$ , respectively. Besides, one state memory cost, the sample number, and the latent feature dimensions denote  $M_S$ ,  $N$ , and  $d$ , respectively. Thus, the time complexity of calculating  $\mathcal{L}_Q$ ,  $\mathcal{L}_{con}$ ,  $\mathcal{L}_{clu}$  is  $O(N_B T_{\mathcal{F}} + N_B N_K / 2 + N_B / 2)$ ,  $O(N^2 d)$ , and  $O(N\hat{K})$ , respectively. In addition, the space complexity of  $\mathcal{L}_Q$ ,  $\mathcal{L}_{con}$ ,  $\mathcal{L}_{clu}$  is  $O(N_B M_S)$ ,  $O(N^2)$ , and  $O(N\hat{K})$ , respectively. The detailed calculation process can be found in Appendix A.4.

## 4 EXPERIMENT

To demonstrate the effectiveness of our proposed Reinforcement Graph Clustering (RGC), we conduct extensive experiments. In the following sections, we introduce the datasets and experimental setups first. And then, we conduct comparison experiments, ablation studies, and analysis experiments.

### 4.1 Dataset

To comprehensively compare our proposed RGC with the state-of-the-art baselines, the experiments are conducted in five benchmark datasets, including CORA [6], CITESEER [1], Amazon Photo (AMAP)[35], Brazil Air-Traffic (BAT)[43] and Europe Air-Traffic (EAT)[43]. The detailed information of datasets are summarized in Table 1 of the Appendix.

### 4.2 Experimental Setup

In our paper, all experiments are conducted on the desktop computer with the Intel Core i7-7820x CPU, one NVIDIA GeForce RTX 2080Ti GPU, 64GB RAM, and the PyTorch deep learning platform. For the compared state-of-the-art baselines, we adopt their source with original settings and reproduce the results. In our method, we train the encoder  $\mathcal{F}$  for 400 epochs. Besides, the quality network  $Q$  is trained for 30 epochs whenever the experience buffer is full. The learning rate of  $Q$  is set to  $1e^{-3}$  and the learning rate of  $\mathcal{F}$  is selected from  $\{1e^{-5}, 1e^{-4}, 1e^{-3}\}$ . Besides, the experience buffer size is searched from  $\{30, 40, 50\}$  and the initial greedy rate  $\epsilon$  is selected from  $\{0.3, 0.5, 0.7\}$ . The initial greedy rate will increase linearly during training. The max cluster number  $N_K$  and the trade-off parameter  $\alpha$  is set to 10. Besides, the discount rate  $\gamma$  is set to 0.1. For the clustering algorithm  $\mathcal{P}$ , we adopt  $K$ -Means and the clustering performance is evaluated by two widely-used metrics, i.e., NMI and ARI [2–4, 15–17].

### 4.3 Clustering Performance Comparison

In this section, we conduct extensive performance comparison experiments to demonstrate the effectiveness of our proposed method.

As shown in Table 2, we first compare our RGC with twenty deep parametric state-of-the-art baselines. Concretely, DEC [66], DCN [67], IDEC [11], and AdaGAE [27] are four representative deep clustering methods. Besides, MGAE [59], DAEGC [58], ARG

**Table 3: Clustering performance of the traditional parametric methods<sup>◦</sup>, traditional non-parametric methods<sup>\*</sup>, and our proposed RGC<sup>‡</sup>. All results are obtained by ten runs and reported with mean $\pm$ std (%). The bold and underlined result denotes the champion and runner-up.**

Method		K-Means <sup>◦</sup>		GMM <sup>◦</sup>	DBSCAN <sup>*</sup>	DPCA <sup>*</sup>	RGC <sup>‡</sup>
		[12]	[51]	[9]	[52]	Ours	
CORA	NMI	26.42+1.03	27.21+1.00	38.46+0.37	14.30+0.40	<b>57.60+1.36</b>	
	ARI	12.97+3.32	<u>15.03+1.02</u>	07.37+1.07	12.42+0.94	<b>49.46+2.72</b>	
	K	-	-	103.0+3.56	<u>15.21+0.84</u>	<b>07.90+1.76</b>	
CITESEER	NMI	<u>34.70+0.66</u>	34.16+0.83	09.01+0.47	14.47+0.87	<b>45.06+0.93</b>	
	ARI	<u>30.72+1.35</u>	30.08+1.40	01.60+0.09	13.24+0.92	<b>46.17+1.46</b>	
	K	-	-	<u>32.67+2.05</u>	45.58+0.24	<b>05.40+0.49</b>	
AMAP	NMI	18.98+1.83	<u>19.74+1.79</u>	17.21+0.03		<b>69.61+0.36</b>	
	ARI	07.83+0.51	07.96+0.68	08.95+0.01	OOM	<b>59.58+0.39</b>	
	K	-	-	<u>7.33+0.47</u>		<b>09.40+0.66</b>	
BAT	NMI	30.50+1.66	30.50+0.00	<u>43.53+0.00</u>	20.92+0.04	<b>51.58+0.83</b>	
	ARI	12.71+0.74	12.71+0.00	<u>36.12+0.02</u>	22.82+0.01	<b>47.16+1.35</b>	
	K	-	-	<u>03.33+0.47</u>	16.02+0.02	<b>03.80+0.60</b>	
EAT	NMI	<u>13.52+1.19</u>	13.52+0.00	09.23+0.40	06.14+0.57	<b>37.77+0.13</b>	
	ARI	02.79+1.54	02.79+0.00	<u>12.39+0.35</u>	07.58+0.26	<b>30.16+0.15</b>	
	K	-	-	<b>04.50+0.24</b>	08.50+0.54	<u>03.30+0.30</u>	

[47], SDCN [1], DFCN [55] are five generative deep graph clustering methods, which reconstruct the attribute or/and topological information. Moreover, AGE [6], MVGRL [13], GDCL [73], GCA [74], MCGC [45], AutoSSL [18], AGC-DRR [10], DCRN [35], AF-GRL [22], ProGCL [61], and SUBLIME [39] are eleven contrastive deep graph clustering methods. They improve the discriminative capability of samples by pulling together the positive samples while pushing away the negative ones. However, previous methods are parametric, and their promising performance heavily relies on the predefined cluster number  $K$ , which is not always available in the real scenario. To solve this problem, we propose RGC by determining the cluster number automatically with reinforcement learning. From the results in Table 2, we have three observations. 1) The deep clustering methods can not achieve promising performance since they merely learn the attribute information while neglecting the graph topological information. 2) Our proposed RGC achieves better performance than the generative methods. The reason is that we adopt the contrastive mechanism, thus improving the discriminative capability of samples. 3) RGC is comparable with the contrastive methods. Here, actually, the comparison is “not fair” since we provide the correct cluster number for the contrastive methods and not for our method RGC. Even under unfair conditions, our proposed RGC is still comparable with state-of-the-art deep parametric methods. The main reason is that the proposed cluster number learning module automatically estimates the cluster number, and the encoder learns the discriminative node embeddings, thus achieving promising performance.

In addition, we also compare our proposed RGC with traditional parametric methods and traditional non-parametric methods. To be specific, two representative traditional parametric methods,  $K$ -Means [12] and GMM [51], adopt the idea of exception maximum to perform clustering. But they still rely on the predefined cluster number. Differently, two traditional non-parameter algorithms DBSCAN [9] and DPCA [52], are free from the predefined cluster number. As shown in Table 3, we have two conclusions as follows. 1) The traditional parametric methods can not achieve promising performance since the representation capability is weak compared

with our method. 2) Although the traditional non-parametric methods, including DBSCAN [9] and DPCA [52], are free from cluster numbers, they are not comparable with ours. The reasons are as follows. Firstly, their representation capability is weaker than the deep methods. Secondly, they are merely designed for the non-graph data and neglect the structural information in graphs.

In summary, our proposed RGC can outperform the traditional parametric/non-parametric methods and achieve comparable performance compared with state-of-the-art deep parametric methods. In the next section, we conduct time cost comparison experiments of our proposed cluster number learning method with the existing cluster number estimation methods.

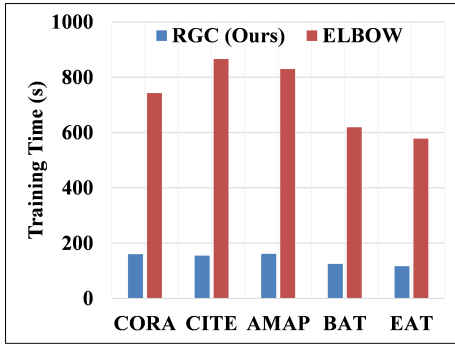


Figure 4: Training time comparison of our proposed RGC and the  $K$  estimation method ELBOW applied to deep graph clustering.

#### 4.4 Time Cost Comparison of $K$ Estimation

The existing deep graph clustering methods are parametric, i.e., relying on the predefined cluster number. In the field of traditional clustering, some cluster number estimation methods like ELBOW [44] can help to determine the cluster numbers. However, it brings large computational costs to the deep graph clustering methods since the deep neural networks need to be trained repeatedly. To verify this, we conduct experiments by comparing the training time of our RGC with that of the  $K$  estimation method. Concretely, for the  $K$  estimation method, we remove the cluster number learning module in RGC and attempt to train the networks with cluster numbers from 2 to  $N_K$ . In Figure 4, the training time of RGC and  $K$  estimation method are visualized. From these results, we conclude that our method is more time efficient than the cluster number estimation method. The main reason is that the  $K$  estimation method requires training the networks repeatedly with different cluster numbers for calculating the unsupervised criterion, such as WSS (within-cluster sum of squares). Only based on the unsupervised criterion calculated by different trained models the  $K$  estimation methods like ELBOW can help to determine the cluster number. Different from them, our cluster number learning module will recognize the cluster number by reinforcement learning. Concretely, the experiences are collected in the process of representation learning and clustering to train the quality network. After optimization, the quality network can automatically determine the cluster number. In these settings, the deep neural networks will be trained only once

in the unified framework of unsupervised representation learning and cluster number determination, thus saving training time.

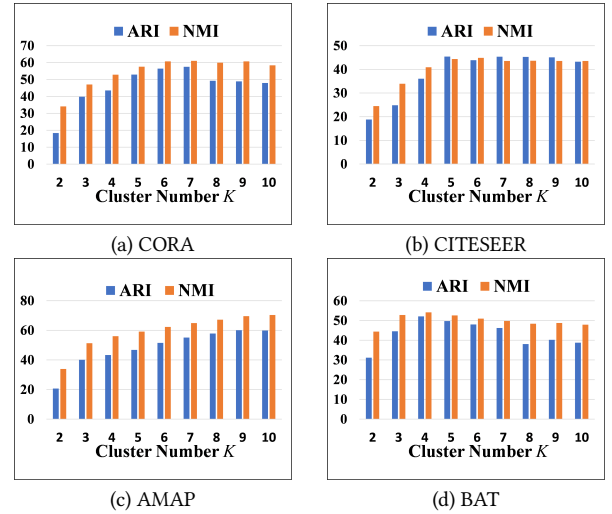


Figure 5: Clustering performance of the baseline trained with different cluster numbers  $K$  on four datasets.

#### 4.5 Effectiveness of Learning Cluster Number

To demonstrate the effectiveness of our proposed cluster number learning module, extensive experiments are conducted.

At first, we demonstrate that the incorrect cluster number will lead to an unpromising performance in deep graph clustering. Concretely, we adopt our RGC without the cluster number learning module as the baseline. Then, the baseline is trained with different cluster numbers from 2 to  $N_K$ . In Figure 5, from these results, we have three conclusions as follows. 1) The wrong cluster number will lead to an unpromising performance in the parametric deep graph clustering methods. Take the results on the CORA dataset, for example, when  $K$  is wrongly assigned to 2, the NMI will rapidly decrease to 34.10%. But, when cluster number  $K$  is 7, the clustering performance NMI can reach 61.05%. 2) The clustering performance is sensitive to different cluster numbers. Take the results on AMAP as an example, the best NMI is 70.40% while the worst NMI is 33.87%. Besides, the standard deviation of NMI with different cluster numbers is 10.81%. 3) The performance will reach the peak around the correct cluster number. But it might not reach the peak exactly at the correct cluster number. For example, on the CORA dataset, the performance reaches a peak at the correct cluster number 7. But on AMAP datasets, NMI reaches a peak at 10, which is around the “correct” cluster number 8. We hope this interesting phenomenon motivates the researchers to discover new classes or design algorithms to find the truly correct cluster number.

Then, we adopt the cluster number estimation method ELBOW [44] to determine the cluster number on CORA and AMAP datasets. Concretely, the baseline is RGC without the cluster number learning module. Besides, the baseline is trained with the cluster number from 2 to  $N_K$ , and the WSS (within-cluster sum of squares) is calculated to determine the cluster number. From the visualization

results in Figure 6, we have three conclusions as follows. 1) The cluster determination based on the unsupervised criterion WSS needs professional experience. For example, on the CORA dataset, we observe that WSS first decrease dramatically when the cluster number equals three and then reaches a plateau. Thus, the cluster number might be wrongly assigned to 3 while the correct cluster number is 7. 2) Besides, the ELBOW method might fail when the trend of WSS is irregular. For example, on the AMAP dataset, the trend of WSS is irregular and we can not find any plateau, leading to the failure of ELBOW.

Different from the cluster number estimation method, our proposed cluster number learning module can automatically determine the cluster number by the reinforcement learning mechanism. In Table 3, we observe that our RGC can recognize the cluster number precisely. For example, on the BAT dataset, the average of our learned cluster number is 3.80 under ten runs, and the ground truth is 4.

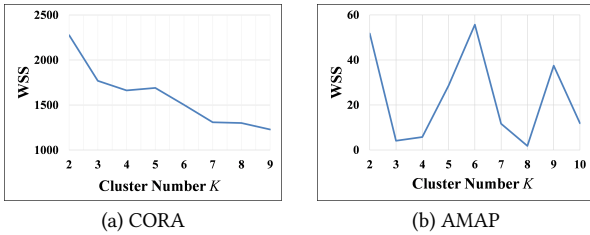


**Figure 6: Determine cluster number with ELBOW [44] cluster number estimation method.**

## 4.6 Analysis

In this section, we conduct analysis experiments for our proposed RGC. To be specific, we analyze the hyper-parameter,  $t$ -SNE visualization, and loss convergence in the following sub-sections.

**4.6.1 Hyper-parameter Analyses.** Due to the page limitation, we conduct hyper-parameters analyses in Appendix.

**4.6.2  $t$ -SNE Visualization Analysis.** We visualize the samples in the latent space by  $t$ -SNE algorithm [56]. As shown in Figure 3, the experiments of seven compared methods are conducted on CORA and AMAP datasets. From the visualization results, our proposed RGC can better learn the clustering structure compared with other methods.

**4.6.3 Loss Convergence Analyses.** Due to the limitation of the main text, the loss convergence analyses are demonstrated in Appendix.

## 5 CONCLUSION

In this paper, we find that the promising performance of the existing deep graph clustering methods heavily relies on the predefined cluster number  $K$ , which is not always known in practice. To solve this open problem, we propose a new deep non-parametric graph clustering method termed Reinforcement Graph Clustering (RGC) by learning the cluster number with reinforcement learning. In RGC, the states are built with both node and cluster embeddings

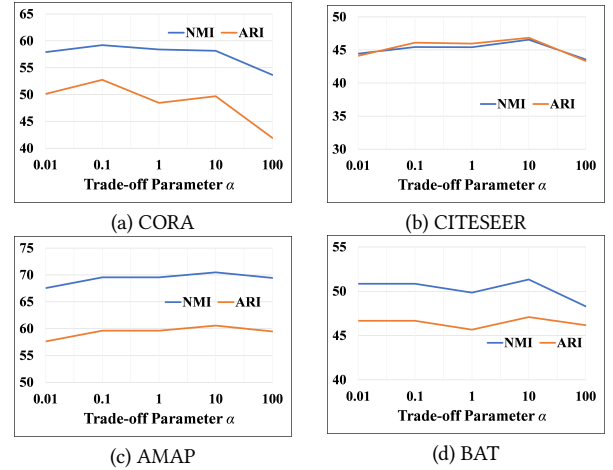


**Figure 7: Hyper-parameter analysis of the trade-off parameter  $\alpha$  on four datasets.**

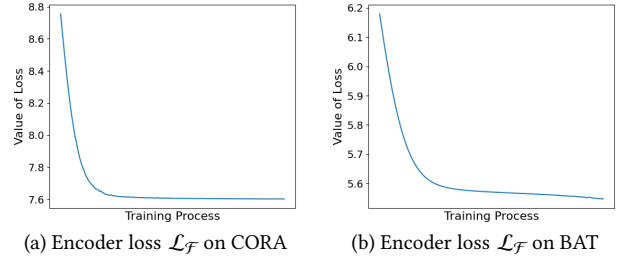


**Figure 8: Loss converge analysis on two datasets.**

to capture the local and global information in the graph. Subsequently, the designed quality network can evaluate the quality of cluster number (action) at the state. Moreover, a clustering-orient reward mechanism is proposed to improve the cohesion of the same clusters while separating the different clusters. In this manner, after optimization, the quality network can automatically determine the cluster number and achieve promising clustering performance. We hope this paper can motivate the researchers to design deeper non-parametric graph clustering methods. In the future, how to determine the cluster number in deep graph clustering methods based on the sample density will be an exciting topic.

## ACKNOWLEDGMENTS

This work was supported by the National Key R&D Program of China 2020AAA0107100 and the National Natural Science Foundation of China (project no. 62325604, 62276271). Besides, this work was also supported by the National Key R&D Program of China (Project 2022ZD0115100), the National Natural Science Foundation of China (Project U21A20427), the Research Center for Industries of the Future (Project WU2022C043), and the Competitive Research Fund (Project WU2022A009) from the Westlake Center for Synthetic Biology and Integrated Bioengineering.



## REFERENCES

- [1] Deyu Bo, Xiao Wang, Chuan Shi, Meiqi Zhu, Emiao Lu, and Peng Cui. 2020. Structural deep clustering network. In *Proceedings of The Web Conference 2020*. 1400–1410.
- [2] Jinyu Cai, Jicong Fan, Wenzhong Guo, Shiping Wang, Yunhe Zhang, and Zhao Zhang. 2022. Efficient deep embedded subspace clustering. In *Proceedings of the IEEE/CVF Conference on Computer Vision and Pattern Recognition*. 1–10.
- [3] Jinyu Cai, Wenzhong Guo, and Jicong Fan. 2022. Unsupervised Deep Discriminative Analysis Based Clustering. *arXiv preprint arXiv:2206.04686* (2022).
- [4] Jinyu Cai, Shiping Wang, Chaoyang Xu, and Wenzhong Guo. 2022. Unsupervised deep clustering via contractive feature representation and focal loss. *Pattern Recognition* 123 (2022), 108386.
- [5] Jiafeng Cheng, Qianqian Wang, Zhiqiang Tao, Deyan Xie, and Quanxue Gao. 2021. Multi-view attribute graph convolution networks for clustering. In *Proceedings of the Twenty-Ninth International Conference on International Joint Conferences on Artificial Intelligence*. 2973–2979.
- [6] Ganqu Cui, Jie Zhou, Cheng Yang, and Zhiyuan Liu. 2020. Adaptive graph encoder for attributed graph embedding. In *Proceedings of the 26th ACM SIGKDD International Conference on Knowledge Discovery & Data Mining*. 976–985.
- [7] Jingcan Duan, Siwei Wang, Xinwang Liu, Haifang Zhou, Jingtao Hu, and Hu Jin. 2022. GADMSL: Graph Anomaly Detection on Attributed Networks via Multi-scale Substructure Learning. *arXiv preprint arXiv:2211.15255* (2022).
- [8] Jingcan Duan, Siwei Wang, Pei Zhang, En Zhu, Jingtao Hu, Hu Jin, Yue Liu, and Zhibin Dong. 2023. Graph anomaly detection via multi-scale contrastive learning networks with augmented view. In *Proceedings of the AAAI Conference on Artificial Intelligence*, Vol. 37. 7459–7467.
- [9] Martin Ester, Hans-Peter Kriegel, Jörg Sander, Xiaowei Xu, et al. 1996. A density-based algorithm for discovering clusters in large spatial databases with noise.. In *kdd*, Vol. 96. 226–231.
- [10] Lei Gong, Sihang Zhou, Xinwang Liu, and Wenxuan Tu. 2022. Attributed Graph Clustering with Dual Redundancy Reduction. In *IJCAI*.
- [11] Xifeng Guo, Long Gao, Xinwang Liu, and Jianping Yin. 2017. Improved Deep Embedded Clustering with Local Structure Preservation.. In *Ijcai*. 1753–1759.
- [12] John A Hartigan and Manchek A Wong. 1979. Algorithm AS 136: A k-means clustering algorithm. *Journal of the royal statistical society. series c (applied statistics)* 28, 1 (1979), 100–108.
- [13] Kaveh Hassani and Amir Hosein Khasahmadi. 2020. Contrastive multi-view representation learning on graphs. In *International Conference on Machine Learning*. PMLR, 4116–4126.
- [14] Xiaochang Hu, Xin Xu, Yujun Zeng, and Xihong Yang. 2023. Patch-Mixing Contrastive Regularization for Few-Label Semi-Supervised Learning. *IEEE Transactions on Artificial Intelligence* (2023), 1–14. <https://doi.org/10.1109/TAI.2023.3247975>
- [15] Sheng Huang, Lele Fu, Yunhe Zhang, Haiping Xu, and Shiping Wang. 2022. Multi-View Deep Matrix Factorization with Consensual Solution from Multiple Paths. In *2022 IEEE International Conference on Multimedia and Expo (ICME)*. IEEE, 1–6.
- [16] Sheng Huang, Yunhe Zhang, Lele Fu, and Shiping Wang. 2022. Learnable Multi-view Matrix Factorization with Graph Embedding and Flexible Loss. *IEEE Transactions on Multimedia* (2022). doi:10.1109/TMM.2022.3157997.
- [17] Jiaqi Jin, Siwei Wang, Zhibin Dong, Xinwang Liu, and En Zhu. 2023. Deep Incomplete Multi-view Clustering with Cross-view Partial Sample and Prototype Alignment. In *Proceedings of the IEEE/CVF Conference on Computer Vision and Pattern Recognition*. 11600–11609.
- [18] Wei Jin, Xiaorui Liu, Xiangyu Zhao, Yao Ma, Neil Shah, and Jiliang Tang. 2021. Automated Self-Supervised Learning for Graphs. In *International Conference on Learning Representations*.
- [19] Thomas N Kipf and Max Welling. 2016. Variational graph auto-encoders. *arXiv preprint arXiv:1611.07308* (2016).
- [20] Thomas N Kipf and Max Welling. 2017. Semi-supervised classification with graph convolutional networks. In *International Conference on Learning Representations*.
- [21] Trupti M Kodinariya and Prashant R Makwana. 2013. Review on determining number of Cluster in K-Means Clustering. *International Journal* 1, 6 (2013), 90–95.
- [22] Namkyeong Lee, Junseok Lee, and Chanyoung Park. 2021. Augmentation-Free Self-Supervised Learning on Graphs. *arXiv preprint arXiv:2112.02472* (2021).
- [23] Liang Li, Siwei Wang, Xinwang Liu, En Zhu, Li Shen, Kenli Li, and Keqin Li. 2022. Local Sample-Weighted Multiple Kernel Clustering With Consensus Discriminative Graph. *IEEE Trans. Neural Networks* (2022), 1–14. <https://doi.org/10.1109/TNNLS.2022.3184970>
- [24] Liang Li, Junpu Zhang, Siwei Wang, Xinwang Liu, Kenli Li, and Keqin Li. 2023. Multi-View Bipartite Graph Clustering With Coupled Noisy Feature Filter. *IEEE Trans. Knowl. Data Eng.* (2023), 1–13. <https://doi.org/10.1109/TKDE.2023.3268215>
- [25] Wang Li, Siwei Wang, Xifeng Guo, Zhenyu Zhou, and En Zhu. 2022. Auxiliary Graph for Attribute Graph Clustering. *Entropy* 24, 10 (2022), 1409.
- [26] Wang Li, Siwei Wang, Xifeng Guo, and En Zhu. 2022. Deep Graph Clustering with Multi-level Subspace Fusion. *Pattern Recognition* (2022), 109077.
- [27] Xuelong Li, Hongyuan Zhang, and Rui Zhang. 2021. Adaptive graph auto-encoder for general data clustering. *IEEE Transactions on Pattern Analysis and Machine Intelligence* (2021).
- [28] Ke Liang, Lingyuan Meng, Meng Liu, Yue Liu, Wenxuan Tu, Siwei Wang, Sihang Zhou, X Liu, and F Sun. 2022. A Survey of Knowledge Graph Reasoning on Graph Types: Static, Dynamic, and Multimodal. (2022).
- [29] Ke Liang, Lingyuan Meng, Sihang Zhou, Siwei Wang, Wenxuan Tu, Yue Liu, Meng Liu, and Xinwang Liu. 2023. Message Intercommunication for Inductive Relation Reasoning. *arXiv preprint arXiv:2305.14074* (2023).
- [30] Ke Liang, Jim Tan, Dongrui Zeng, Yongzhe Huang, Xiaolei Huang, and Gang Tan. 2023. Abslearn: a gnn-based framework for aliasing and buffer-size information retrieval. *Pattern Analysis and Applications* (2023), 1–19.
- [31] Meng Liu, Ke Liang, Yue Liu, Siwei Wang, Sihang Zhou, and Xinwang Liu. 2023. arXiv4TGC: Large-Scale Datasets for Temporal Graph Clustering. *arXiv preprint arXiv:2306.04962* (2023).
- [32] Meng Liu and Yong Liu. 2021. Inductive representation learning in temporal networks via mining neighborhood and community influences. In *Proceedings of the 44th International ACM SIGIR Conference on Research and Development in Information Retrieval*. 2202–2206.
- [33] Meng Liu, Yue Liu, Ke Liang, Siwei Wang, Sihang Zhou, and Xinwang Liu. 2023. Deep Temporal Graph Clustering. *arXiv preprint arXiv:2305.10738* (2023).
- [34] Yue Liu, Ke Liang, Jun Xia, Sihang Zhou, Xihong Yang, Xinwang Liu, and Stan Z. Li. 2023. Dink-Net: Neural Clustering on Large Graphs. In *International Conference on Machine Learning*. PMLR.
- [35] Yue Liu, Wenxuan Tu, Sihang Zhou, Xinwang Liu, Linxuan Song, Xihong Yang, and En Zhu. 2022. Deep Graph Clustering via Dual Correlation Reduction. In *AAAI Conference on Artificial Intelligence*.
- [36] Yue Liu, Jun Xia, Sihang Zhou, Siwei Wang, Xifeng Guo, Xihong Yang, Ke Liang, Wenxuan Tu, Z. Stan Li, and Xinwang Liu. 2022. A Survey of Deep Graph Clustering: Taxonomy, Challenge, and Application. *arXiv preprint arXiv:2211.12875* (2022).
- [37] Yue Liu, Xihong Yang, Sihang Zhou, Xinwang Liu, Siwei Wang, Ke Liang, Wenxuan Tu, and Liang Li. 2023. Simple contrastive graph clustering. *IEEE Transactions on Neural Networks and Learning Systems* (2023).
- [38] Yue Liu, Xihong Yang, Sihang Zhou, Xinwang Liu, Zhen Wang, Ke Liang, Wenxuan Tu, Liang Li, Jingcan Duan, and Cancan Chen. 2023. Hard sample aware network for contrastive deep graph clustering. In *Proceedings of the AAAI conference on artificial intelligence*, Vol. 37. 8914–8922.
- [39] Yixin Liu, Yu Zheng, Daokun Zhang, Hongxu Chen, Hao Peng, and Shirui Pan. 2022. Towards unsupervised deep graph structure learning. In *Proceedings of the ACM Web Conference 2022*. 1392–1403.
- [40] Yue Liu, Sihang Zhou, Xinwang Liu, Wenxuan Tu, and Xihong Yang. 2022. Improved Dual Correlation Reduction Network. *arXiv preprint arXiv:2202.12533* (2022).
- [41] Yingwei Ma, Yue Yu, Shanshan Li, Zhouyang Jia, Jun Ma, Rulin Xu, Wei Dong, and Xiangke Liao. 2023. MulCS: Towards a Unified Deep Representation for Multilingual Code Search. In *2023 IEEE International Conference on Software Analysis, Evolution and Reengineering (SANER)*. IEEE, 120–131.
- [42] Chang Meng, Ziqi Zhao, Wei Guo, Yingxue Zhang, Haolun Wu, Chen Gao, Dong Li, Xiu Li, and Ruiming Tang. 2023. Coarse-to-Fine Knowledge-Enhanced Multi-Interest Learning Framework for Multi-Behavior Recommendation. *ACM Trans. Inf. Syst.* (Jun 2023). <https://doi.org/10.1145/3606369> Just Accepted.
- [43] Nairoz Mrabah, Mohamed Bouguessa, Mohamed Fawzi Touati, and Riadh Ksantini. 2021. Rethinking Graph Auto-Encoder Models for Attributed Graph Clustering. *arXiv preprint arXiv:2107.08562* (2021).
- [44] Andrew Ng. 2012. Clustering with the k-means algorithm. *Machine Learning* (2012), 1–2.
- [45] Erlin Pan and Zhao Kang. 2021. Multi-view contrastive graph clustering. *Advances in neural information processing systems* 34 (2021), 2148–2159.
- [46] Shirui Pan, Ruiqi Hu, Sai-fu Fung, Guodong Long, Jing Jiang, and Chengqi Zhang. 2019. Learning graph embedding with adversarial training methods. *IEEE transactions on cybernetics* 50, 6 (2019), 2475–2487.
- [47] Shirui Pan, Ruiqi Hu, Guodong Long, Jing Jiang, Lina Yao, and Chengqi Zhang. 2018. Adversarially regularized graph autoencoder for graph embedding. In *Proceedings of the 27th International Joint Conference on Artificial Intelligence*. 2609–2615.
- [48] Jiwoong Park, Minsik Lee, Hyung Jin Chang, Kyuewang Lee, and Jin Young Choi. 2019. Symmetric graph convolutional autoencoder for unsupervised graph representation learning. In *Proceedings of the IEEE/CVF International Conference on Computer Vision*. 6519–6528.
- [49] Namyong Park, Ryan Rossi, Eunyee Koh, Iftikhar Ahamath Burhanuddin, Sungchul Kim, Fan Du, Nesreen Ahmed, and Christos Faloutsos. 2022. CGC: Contrastive Graph Clustering for Community Detection and Tracking. In *Proceedings of the ACM Web Conference 2022*. 1115–1126.
- [50] Zhihao Peng, Hui Liu, Yuheng Jia, and Junhui Hou. 2021. Attention-driven Graph Clustering Network. In *Proceedings of the 29th ACM International Conference on Multimedia*. 935–943.

- [51] Douglas A Reynolds. 2009. Gaussian mixture models. *Encyclopedia of biometrics* 741, 659–663 (2009).
- [52] Alex Rodriguez and Alessandro Laio. 2014. Clustering by fast search and find of density peaks. *science* 344, 6191 (2014), 1492–1496.
- [53] Meitar Ronen, Shahaf E Finder, and Oren Freifeld. 2022. DeepDPM: Deep Clustering With an Unknown Number of Clusters. In *Proceedings of the IEEE/CVF Conference on Computer Vision and Pattern Recognition*. 9861–9870.
- [54] Zhiqiang Tao, Hongfu Liu, Jun Li, Zhaowen Wang, and Yun Fu. 2019. Adversarial graph embedding for ensemble clustering. In *International Joint Conferences on Artificial Intelligence Organization*.
- [55] Wenxuan Tu, Sihang Zhou, Xinwang Liu, Xifeng Guo, Zhiping Cai, Jieren Cheng, et al. 2020. Deep Fusion Clustering Network. *arXiv preprint arXiv:2012.09600* (2020).
- [56] Laurens Van der Maaten and Geoffrey Hinton. 2008. Visualizing data using t-SNE. *Journal of machine learning research* 9, 11 (2008).
- [57] Petar Velicković, Guillem Cucurull, Arantxa Casanova, Adriana Romero, Pietro Lio, and Yoshua Bengio. 2017. Graph attention networks. *arXiv preprint arXiv:1710.10903* (2017).
- [58] Chun Wang, Shirui Pan, Ruiqi Hu, Guodong Long, Jing Jiang, and Chengqi Zhang. 2019. Attributed graph clustering: A deep attentional embedding approach. *arXiv preprint arXiv:1906.06532* (2019).
- [59] Chun Wang, Shirui Pan, Guodong Long, Xingquan Zhu, and Jing Jiang. 2017. Mgae: Marginalized graph autoencoder for graph clustering. In *Proceedings of the 2017 ACM on Conference on Information and Knowledge Management*. 889–898.
- [60] Yi Wen, Siwei Wang, Qing Liao, Weixuan Liang, Ke Liang, Xinhang Wan, and Xinwang Liu. 2023. Unpaired Multi-View Graph Clustering with Cross-View Structure Matching. *arXiv preprint arXiv:2307.03476* (2023).
- [61] Jun Xia, Lirong Wu, Ge Wang, Jintao Chen, and Stan Z Li. 2022. ProGCL: Rethinking Hard Negative Mining in Graph Contrastive Learning. In *International Conference on Machine Learning*. PMLR, 24332–24346.
- [62] Jun Xia, Chengshuai Zhao, Bozhen Hu, Zhangyang Gao, Cheng Tan, Yue Liu, Siyuan Li, and Stan Z Li. 2022. Mole-bert: Rethinking pre-training graph neural networks for molecules. In *The Eleventh International Conference on Learning Representations*.
- [63] Lianghao Xia, Chao Huang, Yong Xu, Peng Dai, Xiyue Zhang, Hongsheng Yang, Jian Pei, and Liefeng Bo. 2021. Knowledge-enhanced hierarchical graph transformer network for multi-behavior recommendation. In *Proceedings of the AAAI Conference on Artificial Intelligence*, Vol. 35. 4486–4493.
- [64] Wei Xia, Quanxue Gao, Ming Yang, and Xinbo Gao. 2021. Self-supervised Contrastive Attributed Graph Clustering. *arXiv preprint arXiv:2110.08264* (2021).
- [65] Wei Xia, Qianqian Wang, Quanxue Gao, Xiangdong Zhang, and Xinbo Gao. 2021. Self-supervised graph convolutional network for multi-view clustering. *IEEE Transactions on Multimedia* (2021).
- [66] Junyuan Xie, Ross Girshick, and Ali Farhadi. 2016. Unsupervised deep embedding for clustering analysis. In *International conference on machine learning*. PMLR, 478–487.
- [67] Bo Yang, Xiao Fu, Nicholas D Sidiropoulos, and Mingyi Hong. 2017. Towards k-means-friendly spaces: Simultaneous deep learning and clustering. In *international conference on machine learning*. PMLR, 3861–3870.
- [68] Xihong Yang, Xiaochang Hu, Sihang Zhou, Xinwang Liu, and En Zhu. 2022. Interpolation-Based Contrastive Learning for Few-Label Semi-Supervised Learning. *IEEE Transactions on Neural Networks and Learning Systems* (2022), 1–12. <https://doi.org/10.1109/TNNLS.2022.3186512>
- [69] Xihong Yang, Yue Liu, Sihang Zhou, Xinwang Liu, and En Zhu. 2022. Mixed Graph Contrastive Network for Semi-Supervised Node Classification. *arXiv preprint arXiv:2206.02796* (2022).
- [70] Xihong Yang, Yue Liu, Sihang Zhou, Siwei Wang, Wenxuan Tu, Qun Zheng, Xinwang Liu, Liming Fang, and En Zhu. 2023. Cluster-guided Contrastive Graph Clustering Network. In *Proceedings of the AAAI conference on artificial intelligence*, Vol. 37. 10834–10842.
- [71] Junpu Zhang, Liang Li, Siwei Wang, Jiyuan Liu, Yue Liu, Xinwang Liu, and En Zhu. 2022. Multiple Kernel Clustering with Dual Noise Minimization. In *Proc. of the 30-th ACM Int. Conf. Multimedia, Lisboa, Portugal* (Lisboa, Portugal) (MM '22). New York, NY, USA, 3440–3450. <https://doi.org/10.1145/3503161.3548334>
- [72] Xiaotong Zhang, Han Liu, Qimai Li, and Xiao-Ming Wu. 2019. Attributed graph clustering via adaptive graph convolution. In *Proceedings of the 28th International Joint Conference on Artificial Intelligence*. 4327–4333.
- [73] Han Zhao, Xu Yang, Zhenru Wang, Erkun Yang, and Cheng Deng. 2021. Graph debiased contrastive learning with joint representation clustering. In *Proc. IJCAI*. 3434–3440.
- [74] Yanqiao Zhu, Yichen Xu, Feng Yu, Qiang Liu, Shu Wu, and Liang Wang. 2021. Graph contrastive learning with adaptive augmentation. In *Proceedings of the Web Conference 2021*. 2069–2080.

# Appendix of Paper "Reinforcement Graph Clustering with Unknown Cluster Number"

## ACM Reference Format:

. 2023. Appendix of Paper "Reinforcement Graph Clustering with Unknown Cluster Number". In *Proceedings of Make sure to enter the correct conference title from your rights confirmation email (ACM MM '23)*. ACM, New York, NY, USA, 3 pages. <https://doi.org/XXXXXXX.XXXXXXX>

## APPENDIX

Due to the limited pages of the main body, we introduce some details of our proposed Reinforcement Graph Clustering (RGC) and conduct additional experiments in the following sections.

## A DETAILS OF THE PROPOSED METHOD

In this section, we detail the architecture of encoder  $\mathcal{F}$ , loss function of  $\mathcal{F}$ , the architecture of quality network  $\mathcal{Q}$ , and the calculation process of complexity analysis.

### A.1 Architecture of encoder $\mathcal{F}$

Given the node attributes  $\mathbf{X}$  and the original adjacency matrix  $\mathbf{A}$ , we firstly perform Laplacian filtering for  $\mathbf{X}$  as follow.

$$\tilde{\mathbf{X}} = \left( \prod_{i=1}^t (\mathbf{I} - \tilde{\mathbf{L}}) \right) \mathbf{X} = (\mathbf{I} - \tilde{\mathbf{L}})^t \mathbf{X}, \quad (1)$$

where  $\tilde{\mathbf{L}}$  denotes the symmetric normalized graph Laplacian matrix and  $t$  denotes the filtering times. Subsequently,  $\tilde{\mathbf{X}}$  is embedded by  $\text{Lin}_1$  and  $\text{Lin}_2$  as follows.

$$\begin{aligned} \mathbf{Z}^{v_1} &= \text{Lin}_1(\tilde{\mathbf{X}}); \mathbf{Z}_i^{v_1} = \frac{\mathbf{Z}_i^{v_1}}{\|\mathbf{Z}_i^{v_1}\|_2}, i = 1, 2, \dots, N; \\ \mathbf{Z}^{v_2} &= \text{Lin}_2(\tilde{\mathbf{X}}); \mathbf{Z}_j^{v_2} = \frac{\mathbf{Z}_j^{v_2}}{\|\mathbf{Z}_j^{v_2}\|_2}, j = 1, 2, \dots, N. \end{aligned} \quad (2)$$

Here,  $\mathbf{Z}^{v_1}$  and  $\mathbf{Z}^{v_2}$  denote two-view node embeddings. For  $\text{Lin}_1$  and  $\text{Lin}_2$ , they are both simple MLPs with same architecture but unshared parameters, endow different semantics to two views. Then the output node embeddings can be calculated by linear combination of two views as follow.

$$\mathbf{Z} = (\mathbf{Z}^{v_1} + \mathbf{Z}^{v_2})/2. \quad (3)$$

Permission to make digital or hard copies of all or part of this work for personal or classroom use is granted without fee provided that copies are not made or distributed for profit or commercial advantage and that copies bear this notice and the full citation on the first page. Copyrights for components of this work owned by others than ACM must be honored. Abstracting with credit is permitted. To copy otherwise, or republish, to post on servers or to redistribute to lists, requires prior specific permission and/or a fee. Request permissions from [permissions@acm.org](https://permissions.acm.org).

ACM MM '23, Aug. 6 - 10, 2023, Ottawa, Canada

© 2023 Association for Computing Machinery.

ACM ISBN 978-1-4503-XXXX-X/18/06...\$15.00

<https://doi.org/XXXXXXX.XXXXXXX>

### A.2 Loss function of encoder $\mathcal{F}$

The loss function of training encoder  $\mathcal{F}$  includes two parts, i.e., contrastive loss  $\mathcal{L}_{con}$  and clustering guidance loss  $\mathcal{L}_{clu}$ . To be specific,  $\mathcal{L}_{con}$  is formulated as follows.

$$\mathcal{L}_{con} = \frac{1}{2N} \sum_{j=1}^2 \sum_{i=1}^N \mathcal{L}_i^{v_j}, \quad (4)$$

$$\mathcal{L}_i^{v_j} = -\log \frac{e^{\theta(i^{v_j}, i^{v_l})}}{e^{\theta(i^{v_j}, i^{v_l})} + \sum_{k \neq i} (e^{\theta(i^{v_j}, k^{v_j})} + e^{\theta(i^{v_j}, k^{v_l})})}. \quad (5)$$

where  $j \neq l$ .  $\mathcal{L}_i^{v_j}$  denotes the loss for  $i$ -th node in  $j$ -th view. Besides,  $\theta(\cdot)$  denotes the cosine similarity between the paired samples in the latent space. Namely,  $\theta(i^{v_j}, k^{v_l}) = \mathbf{Z}_i^{v_j} \mathbf{Z}_k^{v_l}$ . By minimizing  $\mathcal{L}_{con}$ , we pull together the same samples in different views while pushing away other samples.

In addition, the clustering algorithm is performed on the node embeddings  $\mathbf{Z}$  and obtain the cluster center  $\mathbf{C} \in \mathbb{R}^{\hat{K} \times d}$  and cluster assignment matrix  $\mathbf{P} \in \mathbb{R}^{N \times \hat{K}}$  as follow.

$$\mathbf{C}, \mathbf{P} = \mathcal{P}(\mathbf{Z}, \hat{K}), \quad (6)$$

where the cluster center  $\mathbf{C}$  is calculated by averaging the node embeddings within each clusters. The clustering guidance loss  $\mathcal{L}_{clu}$  is then formulated as follows.

$$\mathbf{G}_{ij} = \frac{(1 + \|\mathbf{Z}_i - \mathbf{C}_j\|^2)^{-1}}{\sum_{j'} (1 + \|\mathbf{Z}_i - \mathbf{C}_{j'}\|^2)^{-1}}, \quad (7)$$

$$\mathbf{H}_{ij} = \frac{\mathbf{G}_{ij}^2 / \sum_i \mathbf{G}_{ij}}{(\sum_{j'} \mathbf{G}_{ij'}^2) / (\sum_i \mathbf{G}_{ij})}, \quad (8)$$

$$\mathcal{L}_{clu} = KL(\mathbf{G} \parallel \mathbf{H}) = \sum_i \sum_j \mathbf{G}_{ij} \log \frac{\mathbf{G}_{ij}}{\mathbf{H}_{ij}}. \quad (9)$$

Here,  $\mathbf{G}$  and  $\mathbf{H}$  denote the clustering distribution and the sharpened clustering distribution. By minimizing  $\mathcal{L}_{clu}$ , we align the clustering distribution with the sharpened ones, thus improving the cluster cohesion.

In summary, the total loss of encoder  $\mathcal{L}_{\mathcal{F}}$  is formulated as follow.

$$\mathcal{L}_{\mathcal{F}} = \mathcal{L}_{con} + \alpha \mathcal{L}_{clu}, \quad (10)$$

where  $\alpha$  denotes the trade-off hyper-parameter.

### A.3 Architecture of quality network $\mathcal{Q}$

In this section, we detail the network architecture of quality network  $\mathcal{Q}$ . As mentioned in the main body, given the state  $\mathbf{S}_t$ ,  $\mathcal{Q}$  output the quality score vector  $\mathbf{q}_t$  as follow.

$$\mathbf{q}_t = \mathcal{Q}(\mathbf{S}_t) = \mathcal{Q}(\{\mathbf{Z}_t, \mathbf{C}_t\}). \quad (11)$$

<https://doi.org/XXXXXXX.XXXXXXX>

Concretely, we embed the states into the latent space as follow.

$$\begin{aligned} \mathbf{Z}'_t &= \sigma(\text{Norm}(\text{Lin}_{\mathbf{Z}}(\mathbf{Z}_t))), \\ \mathbf{C}'_t &= \sigma(\text{Norm}(\text{Lin}_{\mathbf{C}}(\mathbf{C}_t))), \end{aligned} \quad (12)$$

where,  $\text{Lin}_{\mathbf{Z}}$  and  $\text{Lin}_{\mathbf{C}}$  denote the MLPs for nodes and clusters, respectively. Besides,  $\text{Norm}$  and  $\sigma$  denote normalization and activate function, respectively. Then the node and cluster representations are concatenated together as follow.

$$\mathbf{O}_t = \text{Concat}([\mathbf{Z}'_t, \mathbf{C}'_t]). \quad (13)$$

Eventually, one output layer  $\text{Lin}_{\text{out}}$  and the softmax function are adopted to calculate the quality score vector as follow.

$$\mathbf{q}_t = \text{Softmax}(\text{Lin}_{\text{out}}(\mathbf{O}_t)). \quad (14)$$

By this settings, we firstly embed the collected node and cluster states into the deep latent space and then fusion them to learn the quality of different cluster numbers (actions) for each states. Moreover, after optimization, our RGC can automatically determine the cluster number for the clustering task and achieve promising performance.

#### A.4 Calculation process of complexity analysis

In the main body of this paper, we analysis the time and space complexity of calculating the loss functions in our proposed RGC. Concretely, assume that the max cluster number, the experience buffer size, and the encoding time for one state is  $N_K$ ,  $N_{\mathcal{B}}$ , and  $T_{\mathcal{F}}$ , respectively. Besides, the state memory cost, the node number, and the latent feature dimensions denotes  $M_{\mathcal{S}}$ ,  $N$ , and  $d$ , respectively. Thus, the time complexity of calculating  $\mathcal{L}_Q$ ,  $\mathcal{L}_{con}$ ,  $\mathcal{L}_{clu}$  is  $O(N_{\mathcal{B}}T_{\mathcal{F}} + N_{\mathcal{B}}N_K/2 + N_{\mathcal{B}}/2)$ ,  $O(N^2d)$ , and  $O(N\hat{K})$ , respectively. In addition, the space complexity of  $\mathcal{L}_Q$ ,  $\mathcal{L}_{con}$ ,  $\mathcal{L}_{clu}$  is  $O(N_{\mathcal{B}}M_{\mathcal{S}})$ ,  $O(N^2)$ , and  $O(N\hat{K})$ , respectively.

In this section, we detail the calculation process of the analysis. Firstly, for the Reinforcement learning loss  $Q$ , it is formulated as follow.

$$\mathcal{L}_Q = \frac{1}{t_e - t_s} \sum_{t=t_s}^{t_e-1} (R_t + \gamma \cdot \max Q(\mathbf{S}_{t+1}) - Q(\mathbf{S}_t)[\hat{K}_t])^2. \quad (15)$$

To calculate  $Q$ , we need to encode the states for twice, namely  $Q(\mathbf{S}_{t+1})$  and  $Q(\mathbf{S}_t)$ , costing  $2T_{\mathcal{F}}$  time. Besides, to find the best action at state  $\mathbf{S}_{t+1}$ , it costs  $N_K$  time. Moreover, for other operations like, addition, subtraction and multiplication, they take the constant time cost  $O(1)$ . In summary, for  $N_{\mathcal{B}}$  states in one buffer, the total time costs are formulated as follow.

$$\begin{aligned} O(N_{\mathcal{B}}(2T_{\mathcal{F}} + N_K + 1)) &= \\ O(2N_{\mathcal{B}}T_{\mathcal{F}} + N_{\mathcal{B}}N_K + N_{\mathcal{B}}) &\approx \\ O(N_{\mathcal{B}}T_{\mathcal{F}} + N_{\mathcal{B}}N_K/2 + N_{\mathcal{B}}/2). \end{aligned} \quad (16)$$

During the process, it needs to keep the memory of the buffer, thus costing  $N_{\mathcal{B}}M_{\mathcal{S}}$ . For the contrastive loss  $\mathcal{L}_{con}$ , it is formulated in Eq. (4) and Eq. (5). There, the similarity calculation for each sample pair will cost  $N^2d$  time. Other operations like sum and division cost constant time. Thus, the total time cost of  $\mathcal{L}_{con}$  is formulated as  $O(N^2d)$ . During this process, the memory cost is  $N^2$  since we need to keep the similarities between each sample pair. Furthermore, for the clustering loss  $\mathcal{L}_{clu}$ , it is formulated in Eq. (7), Eq. (8) and Eq. (9). There, it needs to calculate the distance between nodes

with the cluster centers, costing  $N\hat{K}$  time.  $\hat{K}$  is the learned cluster number. Besides, other operations like addition, sum, and division cost constant time. Thus, the time cost of  $\mathcal{L}_{clu}$  is  $O(N\hat{K})$ . In this process, we need to keep the distance between nodes and cluster centers in both  $\mathbf{G}$  and  $\mathbf{H}$ , thus costing  $O(2N\hat{K}) \approx O(N\hat{K})$  memory.

## B ADDITIONAL EXPERIMENTAL RESULT

In this section, we show the detailed statistics of datasets and the additional experimental results.

### B.1 Statistics

The statistics of benchmark datasets are summarized in Table 1.

Table 1: Statistics of six benchmark datasets.

	Dataset	CORA	CITSESEER	AMAP	BAT	EAT
	Type	Graph	Graph	Graph	Graph	Graph
Statistics	# Samples	2708	3327	7650	131	399
	# Dimensions	1433	3703	745	81	203
	# Edges	5429	4732	119081	1038	5994
	# Classes	7	6	8	4	4

### B.2 Hyper-parameter analysis

We analyze the sensitivity of hyper-parameters, including  $\epsilon$  and  $\alpha$  in our proposed RGC. Specifically,  $\epsilon$  is the initial greedy rate and  $\alpha$  denotes the trade-off parameter in  $\mathcal{L}_{\mathcal{F}}$ . As shown in Figure 3, we conduct the sensitivity analysis experiments of hyper-parameter  $\epsilon$  and have two conclusions as follows. 1) Our proposed RGC is not sensitive to the initial greedy rate  $\epsilon$ . It indicates that our method is not sensitive to initialization and will be optimized to achieve good clustering performance. 2) RGC can achieve promising performance when  $\epsilon \in [0.3, 0.7]$ . Thus, in our method, we search  $\epsilon$  in  $\{0.3, 0.5, 0.7\}$ . Besides, as shown in Figure 4, we analyze the trade-off parameter  $\alpha$  on four datasets and have two findings as follows. 1) Our proposed method is not sensitive to the trade-off parameter  $\alpha$  when  $\alpha \in [0.1, 10]$ . 2) RGC will achieve promising performance on CITSESEER, AMAP, and BAT datasets when  $\alpha = 10$ . Thus, in our proposed method,  $\alpha$  is set to 10. The additional experimental results of the sensitivity analysis of hyper-parameter  $\epsilon$  and  $\alpha$  is shown in Figure 1. Similar conclusions with that in the main body of the paper can be obtained on EAT dataset.

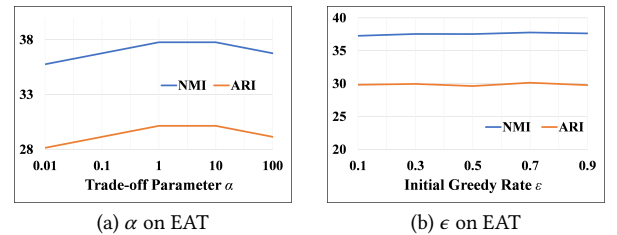


Figure 1: Hyper-parameter analysis of  $\alpha$  and  $\epsilon$  on EAT dataset.

The loss functions of our proposed RGC include two parts, i.e., the encoder loss  $\mathcal{L}_{\mathcal{F}}$  for training encoder  $\mathcal{F}$  and the reinforcement loss  $\mathcal{L}_Q$  for training the quality network  $Q$ . In this section, we plot

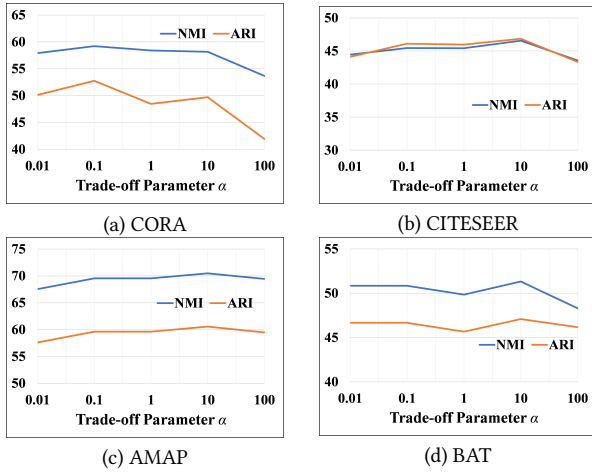


Figure 4: Hyper-parameter analysis of the trade-off parameter  $\alpha$  on four datasets.

the curve of loss functions on two datasets, CORA and BAT, as shown in Figure 2. From these visualization results, the conclusion is that both  $\mathcal{L}_{\mathcal{F}}$  and  $\mathcal{L}_Q$  can decrease during training and eventually converge.

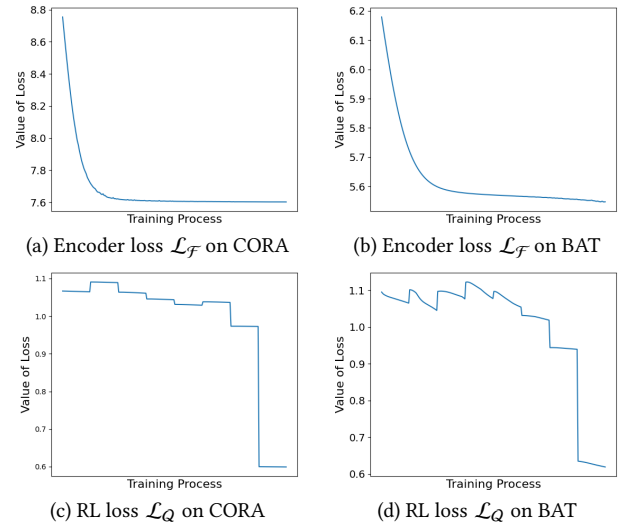


Figure 2: Loss converge analysis on two datasets.



Figure 3: Sensitivity analysis of the initial greedy rate hyper-parameter  $\epsilon$  on four datasets.